Pyrophosphorolysis-Activated Polymerization Detects Circulating Tumor DNA in Metastatic Uveal Melanoma

Jordan Madic[1,2], Sophie Piperno-Neumann[1,3], Vincent Servois[1,4], Aurore Rampanou[1,2], Maud Milder[1,5,6], Bénédicte Trouiller[1,2], David Gentien[1,7], Stéphanie Saada[1,5], Franck Assayag[1,7,8], Aurélie Thuleau[1,7,8], Fariba Nemati[1,7,8], Didier Decaudin[1,7,8], François-Clément Bidard[1,3], Laurence Desjardins[1,9], Pascale Mariani[1,9], Olivier Lantz[1,5,6,10], and Marc-Henri Stern[1,2]

Abstract

Purpose: To develop a molecular tool to detect circulating tumor–derived DNA (ctDNA) in the plasma from patients with uveal melanoma as a marker of tumor burden and monitor treatment efficacy.

Experimental Design: A real-time PCR was developed on the basis of bidirectional pyrophosphorolysis-activated polymerization (bi-PAP) for the quantification of ctDNA using 3′blocked primer pairs specific for the 3 recurrent mutually exclusive mutations of Gα subunits *GNAQ* and *GNA11*.

Results: Sensitivity and specificity of bi-PAP were assessed on serial dilutions of tumor DNA in normal DNA for the 3 recurrent mutations. Each assay could detect a single mutated molecule per reaction, whereas 10^4 copies of normal DNA were not detected. The ctDNA was readily detected in plasma of mice bearing uveal melanoma xenografts in amounts proportional to circulating human DNA. Finally, plasma was almost always found positive (20 of 21 tested patients) in a prospective analysis of patients with metastatic uveal melanoma.

Conclusions: Bi-PAP assays detect and quantify ctDNA in patients with metastatic uveal melanoma. A prospective study is ongoing to assess the clinical usefulness of ctDNA level in uveal melanoma. *Clin Cancer Res; 18(14); 3934–41. ©2012 AACR.*

Introduction

Uveal melanoma is the most common primary intraocular malignancy in adults with an incidence of 6 cases per million per year. Metastatic spread occurs via the hematogenous route and almost invariably involves the liver (1). Despite improvement of diagnosis and treatment of the primary tumor, there is no effective treatment of metastatic disease, and approximately half of patients will die within 1 year or less following metastases detection (2). Several parameters are associated with metastasis and poor survival, including (i) clinical factors such as age, tumor diameter and thickness, extraocular extension, (ii) monosomy 3, and (iii) gene expression profiling after enucleation or fine needle aspiration biopsies of the primary tumor (3–6). An issue in high-risk patients is to detect relapse at the earliest stage after primary tumor treatment. Unfortunately, clinically available methods to assess the extent of the disease such as detection by liver function tests or imaging are generally positive when the metastatic tumor burden is already high (7, 8). Indeed, the detection of small lesions remains a real challenge especially for the miliary form of metastases, which is frequent in uveal melanoma (9). More sensitive methods are needed to assess tumor burden and to improve the monitoring of response to treatment in metastatic patients. Such tools could be also very useful to detect disease recurrence at an early stage to select patients who may benefit the most from adjuvant therapies.

Circulating cell-free DNA (cfcDNA) represents such a suitable marker and several studies have shown its presence in human blood in various malignancies (for a review, see ref. 10). In patients with cancer, the circulating tumor DNA (ctDNA) represents a fraction of cfcDNA bearing the same genetic and epigenetic alterations than the related primary tumor. The majority of ctDNA is derived from tissue tumor cells rather than from circulating tumor cells (CTC) and even primary tumors have been shown to release ctDNA in the bloodstream (11). A milestone contribution from Diehl and colleagues was the demonstration that detection and quantification of specific mutations in ctDNA fragments could be successfully used to assess tumor burden and monitor treatment efficacy in colorectal carcinomas (12).

Authors' Affiliations: [1]Institut Curie; [2]INSERM U830; Départements [3]d'Oncologie Médicale, [4]d'Imagerie Médicale, [5]Biologie des Tumeurs, [6]CIC-BT-507 INSERM; [7]Département de Recherche Translationnelle, [8]Laboratoire d'Investigation Préclinique, [9]Département de Chirurgie, and [10]INSERM U932, Paris, France

O. Lantz and M.-H. Stern contributed equally to this article.

Corresponding Authors: Marc-Henri Stern, Institut Curie, INSERM Unit 830, 26 rue d'Ulm 75248 Paris cedex 05, France. Phone: 33-1-56246646; Fax: 33-1-56246630; E-mail: marc-henri.stern@curie.fr; and Olivier Lantz, Institut Curie, Laboratory of Immunology and INSERM Unit 932, 26 rue d'Ulm 75248 Paris cedex 05, France. Phone 33-1-44324218, Fax 33-1-53102652; E-mail: olivier.lantz@curie.net

American Association for Cancer Research

Translational Relevance

Despite continuous improvement in primary tumor treatment, prognosis of metastatic uveal melanoma (MUM) remains dismal. It is likely that adjuvant therapies will benefit more to patients with low tumor burden, but imaging and biologic tools are rather insensitive and positive only in metastatic patients with high tumor mass. We thus aimed to detect disseminated disease at early stage by evaluating circulating blood tumor DNA taking advantages of the highly recurrent *GNAQ/11*[Q209] mutations in this disease, and the pyrophosphorolyis-activated polymerization (PAP) technique; an exquisitely sensitive and specific molecular technique derived from the PCR. We here show that PAP detects a single mutated molecule among 10^4 genome equivalent of normal DNA and detected tumor DNA in all GNAQ/11-mutated uveal melanoma xenograft models. More importantly, PAP was positive in plasmatic DNA for 20 of 21 patients with MUM and quantification of tumor DNA correlated well with metastasis volume estimated by imaging. This new technique, which required no special equipment, may enable the selection of patients with minimal tumor mass and facilitate the early evaluation of therapeutic efficiency.

Several issues concerning sample processing, assay specificity, and sensibility remain to be addressed. The main difficulty is to set up techniques enabling detection and quantification of tumor-specific single base changes in a large excess of wild-type DNA. For example, PCR-based methods using 5′ hydrolysis probes fail to detect less than 1% mutant DNA diluted in normal DNA (13). To overcome this problem, digital PCR methods compartmentalize the cfcDNA fragments through water-in-oil emulsion (BEAMing) or using a droplet-based microfluidic system before individual analysis and quantification (11, 14, 15). However, these strategies remain delicate and expensive to conduct, requiring instrumentations and expertise beyond most diagnostic laboratory settings. A promising method developed by Sommer and colleagues relies on the use of PAP, a highly specific PCR-derived method that can detect point mutations in the presence of a great excess of wild-type DNA (16, 17). The specificity of this method, which totally discriminates a single nucleotide change, derives from the serial coupling of activation of 2 opposing 3′-blocked pyrophosphorolysis activatable oligonucleotides (bi-PAP) with extension of the unblocked oligonucleotides (18; Fig. 1). These blocked oligonucleotides must perfectly anneal to their complementary target for their activation to occur, limiting the risk of false-positive and self-dimerization.

The present study describes the development and the validation of a bi-PAP real-time PCR approach for the detection of tumor-specific mutations in cfcDNA of patients with uveal melanoma. More than 80 % of patients with uveal melanoma have mutually exclusive somatic mutations in *GNAQ* or its paralog *GNA11*, both genes encoding α-subunits of heterotrimeric G proteins (19, 20). Mutations occur almost exclusively at nucleotide 626, leading to substitution of the glutamine at codon 209 into a leucine for *GNAQ*[626A>T] (Glu209Leu) and *GNA11*[626A>T] (Glu209-Leu), or a proline for *GNAQ*[626A>C] (Glu209Pro), and turning *GNAQ* and *GNA11* into dominant-acting oncogenes. These mutations are not clearly associated to a poor prognosis (21). These mutations are thought to occur at the early
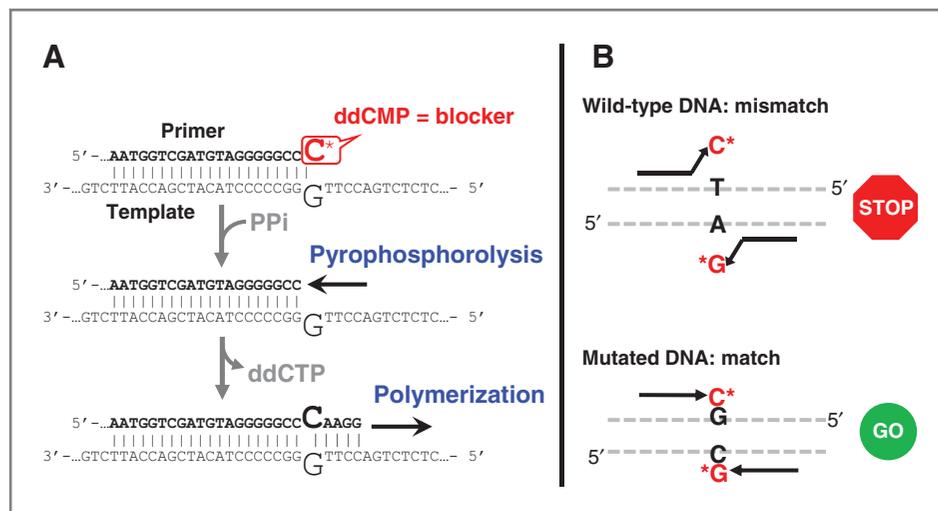

Figure 1. Principle of PAP detection technique. A, from top to bottom. A primer blocked at its 3′ extremity by a dideoxynucleotide anneals specifically to its complementary target. In presence of pyrophosphate, the dideoxynucleotide is removed by the pyrophosphorolytic activity of the polymerase. The unblocked primer can then be extended by polymerization. B, bidirectionnal PAP (bi-PAP) amplification. Two opposing blocked primers overlapping by one nucleotide at their 3′ termini cannot be directly activated and extended by DNA polymerase if mismatched. In presence of the mutated target matching the primers, the blockers are removed by pyrophosphorolysis, enabling specific PCR amplification.

phase of oncogenesis as they are also found in benign proliferations of melanocytic origin, such as blue nevus and nevus of Ota (19, 20).

To detect and quantify these mutations in ctDNA, 3 bi-PAP assays targeting $GNAQ^{626A>T}$, $GNAQ^{626A>C}$, and $GNA11^{626A>T}$ were designed. These assays were validated in terms of sensitivity and specificity in reconstruction experiments and plasma from xenografted mice. More importantly, these assays allowed a quantitative detection of ctDNA in plasma from patients with metastatic uveal melanoma (MUM).

Materials and Methods

Biologic samples

Uveal melanoma xenografts established at Institut Curie (Paris, France) are described previously (22). The following 11 xenografts models were used in this study: MM26, MM33, MM52, MM66, MP34, MP38, MP41, MP42, MP46, MP55, and MP80. In addition, a cell line derived for a uveal melanoma xenograft (MP65) was used for set up. Peripheral blood samples (100–500 μL) were drawn into EDTA tubes at different stages of engraftment. Tumor size was measured at time of the sampling.

Human blood samples (15 mL) were collected in EDTA tubes from a series of 21 patients with a confirmed diagnosis of MUM, at distance (more than 6 months) of any invasive exploration and systemic treatment for 16 patients, 3 weeks after chemotherapy for 3 patients, one week after liver biopsy for a patient, and 2 months after liver surgery for another patient. The primary tumor has either been surgically removed or treated by brachytherapy or proton therapy and locally controlled in all cases. Patients were prospectively enrolled in this study at any time of the metastatic disease course. The protocol was approved by Ethical and Clinical committees and all patients signed an informed consent. Blood samples from 20 healthy human individuals were used as control.

Plasma preparation and DNA extraction

Plasma samples were prepared as described by Diehl and colleagues (12). Briefly, blood was centrifuged at $820 \times g$ for 10 minutes. The supernatant was transferred to sterile tubes, centrifuged at $16,000 \times g$ for 10 minutes at room temperature, and the supernatant was stored at $-80°C$. The overall process from blood collection to plasma storage did not exceed 3 hours. DNA was extracted from plasma of patients and xenografts using the QIAamp Circulating Nucleic Acid and MinElute Virus Vacuum Kits (Qiagen), respectively. Extraction was conducted according to the manufacturer's instructions except that only 1 μg RNA carrier was used. Nucleic acids were stored at $-20°C$.

Mutation screening of GNAQ and GNA11 in tumors and xenografts

For tumors, one microgram of RNA was reverse-transcribed using SuperScript II Reverse Transcriptase (Life Technologies). A 300-bp region was amplified from tumor cDNA or xenograft DNA using the following primer set: GNAQ_Fwd, 5-GATGTGCTTAGAGTTCGAGTCC-3′, GNAQ_Rev, 5′-TTCTCATTGTCTGACTCCACGA-3′, GNA11_Fwd 5′-TACCAGCTCTCCGACTCTGC-3′, and GNA11_Rev, 5′-TTGGTCGTATTCGCTGAGG-3′. Purified PCR products were sequenced with dideoxynucleotides (BigDye Terminator v1.1, Life Technologies), 3.2 pmol of specific primer in 20 μL, purified on a Sephadex G50 column, and analyzed with a capillary sequencing machine (3500xl Genetic Analyzer, Life Technologies).

Real-time PCR assays

In bi-PAP real-time PCR assays, primers blocked at their 3′ termini by a dideoxynucleotide (dd) and specific for $GNAQ^{626A>T}$ Fwd, 5′-ACCTTGCAGAATGGTCGATGTAGGGGGCC-ddT-3′, $GNAQ^{626A>T}$ Rev, 5′-AGTGTATCCATTTTCTTCTCTCTGACCTT-ddA-3′, $GNAQ^{626A>C}$ Fwd, 5′-ACCTTGCAGAATGGTCGATGTAGGGGGCC-ddC-3′, $GNAQ^{626A>C}$ Rev, 5′-AGTGTATCCATTTTCTTCTCTCTGACCTT-ddG-3′ and $GNA11^{626A>T}$ Fwd, 5′-TCCTTTCAGGATGGTGGATGTGGGGGGCC-ddT-3′ and $GNA11^{626A>T}$ Rev, 5′-AGTGGATCCACTTCCTCCGCTCCGACCGC-ddA-3′ were obtained from Eurogentec and Biosearch Technologies. The PCR reaction was done in a total volume of 25 μL including DNA sample, 1 U KlenTaq-S (Scientech Corp), 1X KlenTaq-S buffer, 8% (v/v) dimethyl sulfoxide (DMSO), 25 μmol/L of each dNTP, 1 mmol/L dithiothreitol (DTT), 0.1X ROX calibration dye, 0.2X SYBR Green I dye (Life Technologies), and optimized concentrations of primers and Na_4PPi as follows: the PCR assay targeting $GNA11^{626A>T}$ and $GNAQ^{626A>T}$ contained 5 pmol of each primer, and 30 or 40 μmol/L Na_4PPi, respectively. The PCR assay targeting $GNAQ^{626A>C}$ contained 2.5 pmol of each primer and 30 μmol/L Na_4PPi. The cycling conditions consisted of an initial denaturation step at 94°C for 2 minutes followed by 40 to 45 cycles of 94°C for 20 seconds, 60°C for 30 seconds, 64°C for 30 seconds, and 72°C for 30 seconds. The final step involved the generation of a melting curve analysis.

Total human cfcDNA was quantified using the LINE1 real-time PCR assay (LINE1 PCR) as described in Rago and colleagues (23). A serial dilution of normal human peripheral blood mononuclear cells (PBMC) DNA was incorporated in each plate as standard. All real-time PCR assays were carried out in a 7500 Fast Real-Time PCR System (Life Technologies). The baseline and the cycle threshold value (C_t) were set using the Life Technologies software.

Efficiency, sensitivity, and specificity of the bi-PAP real-time PCR assays

DNA extracted from uveal melanoma xenografts or cell lines (MM33, MP38, and MP65) and from PBMCs were used as positive and negative controls, respectively. DNA concentration was determined by spectrophotometry using a NanoDrop 2000c apparatus. The diploid genome equivalent (GE) was calculated assuming a DNA content of 6.6 pg per cell. Specificity and sensitivity were determined on reconstruction experiments with serial dilutions of tumor DNA ($1–10^4$ GE) in 10^4 GE of normal human PBMC DNA.

Quantitative detection of ctDNA in human samples

DNA was extracted from 5 mL plasma and eluted in a final volume of 36 µL. Bi-PAP PCR assays were conducted on 10 µL DNA in 3 independent experiments. The sensitivity and the specificity of the assays were controlled on each plate by using serial dilutions of tumor DNA in normal DNA, including 10 replicates of mixtures containing 1 GE of the targeted genes and 6 replicates of 10^4 GE of normal DNA, respectively.

Estimation of liver metastasis volume by imaging

The volume of the metastatic lesions was estimated on liver MRIs containing morphologic T1 and T2 sequences, T1 dynamic sequences after injection of a gadolinium chelate as well as a diffusion-weighted sequence with respiratory synchronization, and conducted near the time of blood sampling. For each patient ($n = 16$) with nodular lesions, all the round and well-limited lesions were manually measured. Their volume was calculated according to the formula of the volume of a sphere. For the patients ($n = 5$) presenting lesions with irregular shape, ill-defined borders or too numerous, the volume was calculated on the sequence of imaging offering the best contrast with the healthy liver on a dedicated imaging workstation by means of a thresholding method.

Statistical analysis

Statistical analyses were conducted using GraphPad Prism version 5.0. Correlation between the log-transformed variables were estimated using linear regression models (Pearson) and confirmed using a nonparametric Spearman test. Mann–Whitney U test was used to compare cfcDNA concentration between patients with MUM and control group. P values lower than 0.05 were considered statistically significant.

Results

Features of the bi-PAP real-time PCR assays

We developed 3 bi-PAP assays to detect the 3 most recurrent $GNAQ$ and $GNA11$ point mutations in uveal melanoma. Primer pairs were designed to target a short DNA sequence (<60 bp), as detection of short amplicon (<100 pb) has been shown to be more suitable for tumor DNA detection in plasma (ctDNA; ref. 24). Efficiency, linearity, sensitivity, and specificity of the bi-PAP assays were assayed in reconstruction experiments in which tumor DNAs carrying the targeted mutations were serially diluted in a background of 10^4 GE of normal DNA. Linearity ranged over a 3-log from 10^4 to 10 copies of targets per reaction, allowing quantitative detection. Efficiency was 74, 90, and 100%, for $GNAQ^{626A>T}$, $GNAQ^{626A>C}$, and $GNA11^{626A>T}$, respectively (Fig. 2). The suboptimal efficiency observed in one assay might be related (i) to the opposite direction of the pyrophosphorolysis and polymerization reactions and the necessary addition of PPi, which inhibit the polymerization; (ii) to the specific sequence encompassing the detected mutation; (iii) to suboptimal quality of the primers

as 3′-blocked primers are difficult to synthesize. To further determine the limit of detection and specificity of the bi-PAP assays, 10 replicates containing 5, 2.5, 1, and 0 copies of the target genes in 10^4 GE of normal DNA were assessed. The results are summarized in Table 1. Bi-PAP achieved a high sensitivity in all 3 assays. Five copies of the targets were consistently detected for $GNAQ^{626A>T}$, $GNAQ^{626A>C}$, and in 8 of 10 assays for $GNA11^{626A>T}$, whereas 2.5 copies were detected in 8, 10, and 7 of 10 assays for $GNAQ^{626A>T}$, $GNAQ^{626A>C}$, and $GNA11^{626A>T}$, respectively. A single copy of the target was detected in 6 of 10 replicates with the $GNAQ^{626A>T}$ and $GNA11^{626A>T}$ bi-PAP assays and 4 of 10 replicates with the $GNAQ^{626A>C}$ bi-PAP assay. These results are compatible with a Poisson distribution, and indicate a sensitivity of 1 copy per reaction. No positive detection occurred when cross-testing tumor DNAs and the 3 bi-PAP assays specific for the irrelevant $GNAQ/GNA11$ mutations (data not shown). Finally, no positive detection was observed for the 3 assays in 10 replicates containing only 10^4 GE of normal DNA. Some signal was observed at the last PCR cycles for the $GNA11^{626A>T}$ assay, but with a high C_t and a different melting temperature.

Validation of the bi-PAP real-time PCR assays on plasma of mice bearing xenografts

We then assessed the ctDNA detection assays in experimental models of uveal melanoma. A total of 11 xenografts were tested for their $GNA11/GNAQ$ mutations. The $GNA11^{626A>T}$ mutation was found in 6 xenografts models, whereas $GNAQ^{626A>C}$ and $GNAQ^{626A>T}$ mutations were found in 2 models, respectively. No mutation was found in the MM52 model. At time of sacrifice, the tumor was measured and plasma collected for DNA extraction. Plasma DNAs were then assayed with the LINE1 PCR assay for human cfcDNA detection and the 3 bi-PAP PCR assays for the detection of $GNAQ/GNA11$-activating mutations. Human cfcDNA concentration ranged from 1 to 152 GE per 20 µL of plasma in xenografted mice. In 6 ungrafted mice, cfcDNA concentration ranged from 0.056 to 0.136 GE per 20 µL of plasma, representing either some nonspecific amplification of murine DNA or an unavoidable very low level of human DNA contamination (23). Mutations targeted by the 3 bi-PAP assays were detected in plasma DNAs extracted from all the xenografts according to their mutational status. No positive detection was observed with the 3 bi-PAP assays on plasma from MM52 and ungrafted mice. As expected, cfcDNA and ctDNA concentration measured in plasma were positively correlated (Fig. 3) further validating the bi-PAP assays.

Quantitative detection of GNAQ/GNA11 mutations in MUM patients

We then explored whether bi-PAP assays detect ctDNA in human samples. A series of 21 patients with MUM were prospectively assessed for ctDNA. Activating $GNAQ/GNA11$ mutations were determined by bi-PAP on tumor biopsies, and the relevant bi-PAP assay was conducted on the corresponding plasma samples. In one case, for which no tumor
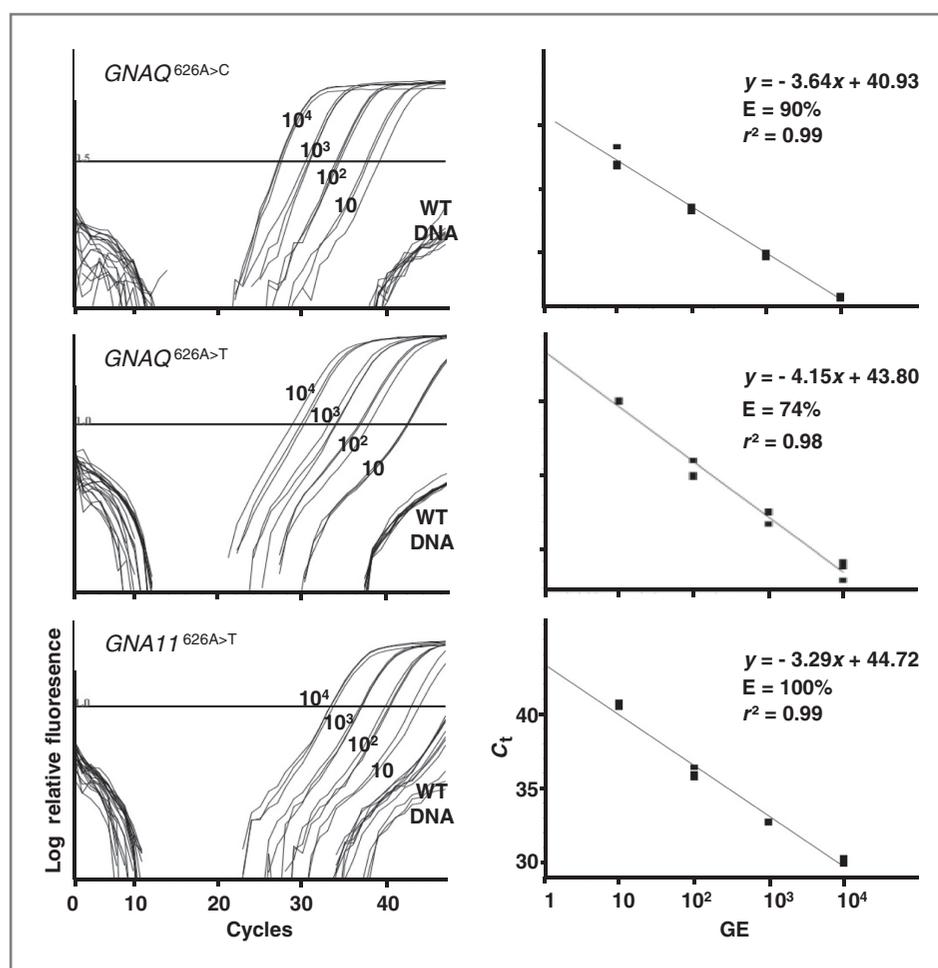
Figure 2. Efficiency of bi-PAP real-time PCR assays. The 3 bi-PAP assays were evaluated in reconstruction experiments. Left, representative amplification plots obtained for admixture of tumor DNAs harboring $GNAQ^{626A>C}$, $GNAQ^{626A>T}$, and $GNA11^{626A>T}$ at 10^4, 10^3, 10^2, 10^1, and 0 (WT DNA) copies in 10^4 GEs of normal DNA. Right, corresponding standard curves generated by plotting the log of GEs per assay (x-axis) versus the C_t value (y-axis).

sample was available, the bi-PAP assays were directly conducted on plasma DNA. The cfcDNA was measured by LINE-1 PCR allowing the calculation of the proportion of ctDNA in plasma cfcDNA. The activating mutations were detected in all but one (20 of 21) plasma samples from patients with MUM, whereas no positive detection was observed in plasma of 20 healthy volunteers. High variations of ctDNA amount were found among patients (Fig. 4) ranging from 1.3 to 2,125 copies per mL of plasma and representing 0.08% to 100% of the total cfcDNA. In 6 patients with advanced MUM (#8, 9, 10, 13, 18, and 19), the ctDNA fraction reached 19.2 to 100% of the total cfcDNA. The weak correlation found between ctDNA and cfcDNA levels (Supplementary Fig. S1 and Supplementary Table S1) was mainly due to these advanced cases, and cfcDNA distribution largely overlapped between patients with MUM and controls. Thus, cfcDNA is of no apparent clinical value in uveal melanoma. In some cases, very low amount of ctDNA was measured, highlighting the need to conduct ctDNA quantification on large volume of plasma.

Table 1. Sensitivity and specificity of the 3 bi-PAP assays

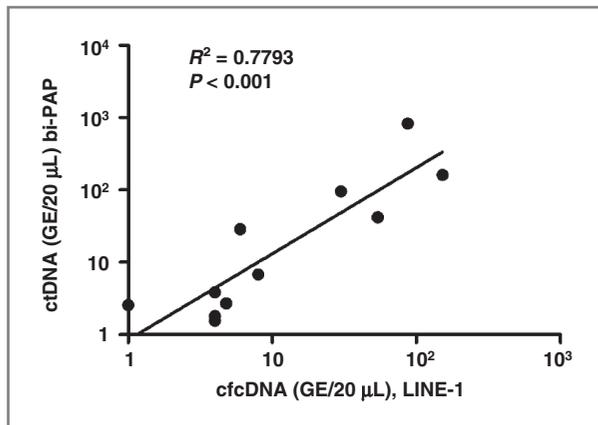| Mutants:WT[a]	Positive detection/nb assays			Expected positivity according to a Poisson distribution
	$GNAQ^{626A>T}$	$GNAQ^{626A>C}$	$GNA11^{626A>T}$	
5:10,000	10/10	10/10	8/10	99%
2.5:10,000	8/10	10/10	7/10	91%
1:10,000	6/10	4/10	6/10	63%
0:10,000	0/10	0/10	0/10	0

[a]In GEs.

Figure 3. Correlation between cfcDNA and ctDNA in xenografted mice. cfcDNA and ctDNA levels in plasma of xenografted mice for 11 independent models of uveal melanoma. Human cfcDNA and *GNAQ/11*-mutated ctDNA were quantified by LINE-1 PCR assay and bi-PAP PCR assays, respectively.

Even using these large amounts of cfcDNA, ctDNA were found in some instance below 5 copies, leading to Poisson distribution with the risk of false negative as exemplified in cases #4 and 7. Variability displayed among the replicates observed in patients #1, 11, 17, and 21 might be explained by technical issues or potential presence of inhibitors in samples, which represents a caveat of assessing large volume of biologic material.

Correlation between ctDNA and tumor burden as assessed by imaging

CtDNA levels are probably related to both tumor burden and tumor cell death rate. We therefore looked for a possible correlation between ctDNA, as measured by bi-PAP and tumor burden assessed by liver MRI. Figure 5 shows a linear relationship between the 2 variables ($R^2 = 0.5827$; $P < 0.001$), indicating that the main determining factor of ctDNA is tumor mass. Noteworthy, the only patient with no detectable ctDNA had a low tumor burden with a liver metastasis volume estimated at 0.46 cm^3. Therefore, ctDNA represents a potential biomarker for tumor burden assessment.

Discussion

This study shows that PAP developed over years by Sommer and Colleagues is a reliable, exquisitely sensitive, and specific technique able to detect circulating tumor DNA identified by a single nucleotide variation (16, 17). An important advantage of PAP over other proposed techniques is its simplicity, allowing its implementation in most clinical molecular pathology laboratories. Once the assay has been set up, the per sample cost is low, enabling longitudinal studies of large cohorts. All recurrent (mostly activating) oncogenic mutations could potentially be assessed by PAP; uveal melanoma representing a remarkable model situation in which 3 mutations encompass 85% of patients. Other biomarkers of dissemination have been

proposed in uveal melanoma, mainly based on the detection of CTCs either by quantitative real-time PCR (25, 26), or by magnetic immunopurification followed by immunohistochemistry (27, 28). However, illegitimate transcription could cause false-positive results using real-time PCR and CTC immunopurification/immunohistochemistry is costly, labor intensive, and requires a trained pathologist. Comparisons of ctDNA and CTC assessments in large uveal melanoma cohorts will be necessary to determine the respective significance and clinical usefulness of both strategies.

PAP assay was shown to be consistently positive in MUM and is an easy and reliable measure of tumor burden. In this disease, local eradication is achieved in the vast majority of cases, and subsequent presence of ctDNA is likely to reflect metastatic disease. However, one cannot exclude that the irradiated ocular tumor tissues could release ctDNA for a long period of time. A prospective longitudinal study
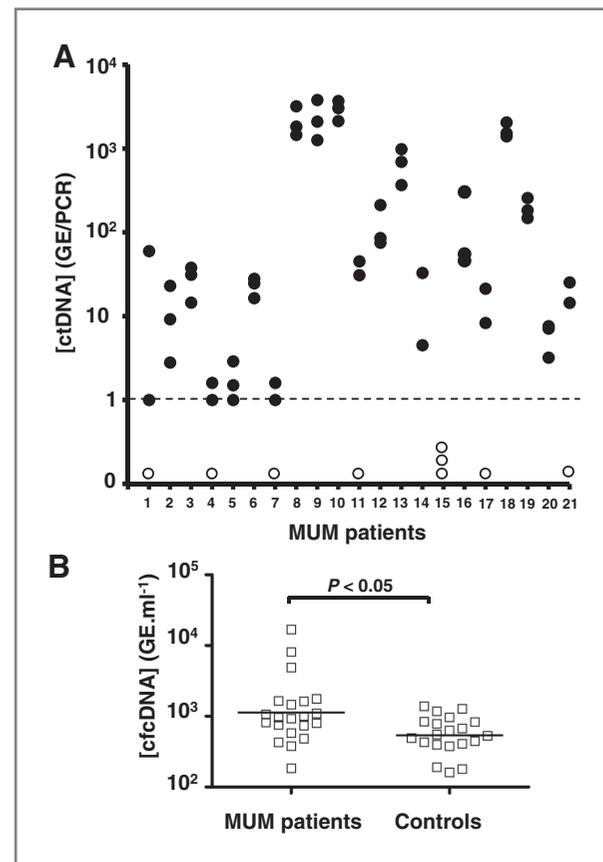

Figure 4. CtDNA and cfcDNA level in patients with MUM. A, ctDNA concentrations expressed as GE per reaction (GE/PCR) in plasma samples of 21 patients with MUM measured by bi-PAP assay in 3 independent experiments. Positive replicates are represented as plain circles. Dashed line represents the limit of sensitivity of the bi-PAP assay and empty circle below the dashed line represents negative replicates. B, cfcDNA concentration measured by LINE1 PCR assay in plasma samples of 21 patients with MUM and in 20 healthy volunteers. Geometric mean is represented by a bar, and the *P* value of the Mann–Whitney *U* test is indicated. GE.mL^{-1}, GE per mL.
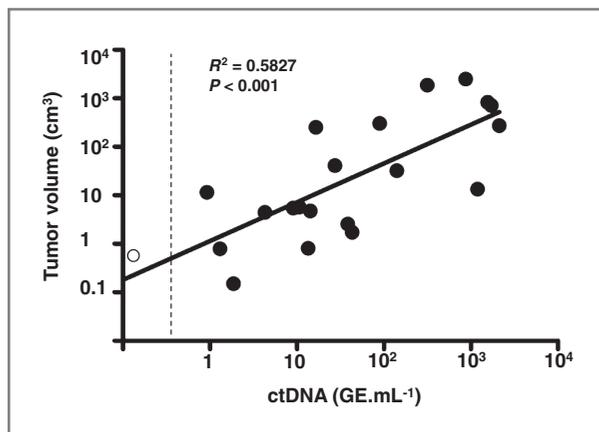
Figure 5. Correlation between ctDNA and tumor burden assessed by MRI. ctDNA levels in $GE.ml^{-1}$ in plasma of 21 patients with MUM were correlated with the volumes of liver metastases in cm^3 as assessed by MRI. Dashed line represents the limit of sensitivity of the bi-PAP assay and empty circle below the dashed line represents the negative bi-PAP assay.

analyzing patients undergoing brachy or proton therapies is required to address this possibility. Therefore, at the present time, the presence of ctDNA cannot be used to ascertain a disseminated disease.

In 2 patients with low tumor burden, we observed negative replicates reflecting the stochastic nature of the bi-PAP assay. This highlights the need to process large quantity of biologic material to lower the limit of detection. However, this may lead to the presence of polymerase inhibitors, which should be minimized by optimizing DNA extraction and purification protocol. In addition, false-negative replicates were observed especially during the implementation of the technique in patients with high copy level (patients #11, 17, and 21), and were probably due to technical issues. These issues are now fully controlled by conducting replicates in independent experiments and by verifying the sensitivity of the bi-PAP in every experiment. This includes low and high positive controls, 10 replicates at 1 copy per reaction and several negative controls.

Large prospective studies measuring ctDNA inpatients with uveal melanoma are required to assess the clinical usefulness of this biomarker at different stages of the disease: (i) at primary diagnosis and after treatment of the primary tumor to assess the prevalence of ctDNA at early stage and its prognostic significance; (ii) during follow-up in high-risk patients to assess the respective sensitivity of ctDNA detection versus imaging for early detection of

metastatic dissemination; (iii) during treatment of the metastatic disease to assess tumor lysis potentially induced by chemotherapy and tumor burden evolution during treatment; and (iv) before liver surgery to select patient candidates to R0 (microscopically complete) resection of liver metastases.

New targeted therapies are being developed in uveal melanoma. Once signs of clinical efficacy have been showed in metastatic patients, ctDNA could be used to select patients with micrometastatic disease to be included into future clinical trials in an adjuvant setting. Noteworthy, the bi-PAP technique is applicable to any recurrent oncogenic mutations such as in *PI3K*, *KRAS*, and *BRAF*. Once developed, this inexpensive assay could be used in a wide variety of frequent cancers, such as breast, colorectal, and pancreatic carcinomas or cutaneous melanoma.

Disclosure of Potential Conflicts of Interest

No potential conflicts of interest were declared by the authors.

Authors' Contributions

Conception and design: B. Trouiller, L. Desjardins, O. Lantz, M.-H. Stern
Development of methodology: J. Madic, A. Rampanou, B. Trouiller, O. Lantz, M.-H. Stern
Acquisition of data (provided animals, acquired and managed patients, provided facilities, etc.): S. Piperno-Neumann, V. Servois, M. Milder, D. Gentien, F. Assayag, A. Thuleau, F. Némati, D. Decaudin, F.-C. Bidard, L. Desjardins, P. Mariani
Analysis and interpretation of data (e.g., statistical analysis, biostatistics, computational analysis): J. Madic, V. Servois, A. Rampanou, P. Mariani, O. Lantz, M.-H. Stern
Writing, review, and/or revision of the manuscript: J. Madic, S. Piperno-Neumann, V. Servois, A. Rampanou, D. Gentien, F.-C. Bidard, O. Lantz, M.-H. Stern
Administrative, technical, or material support (i.e., reporting or organizing data, constructing databases): A. Rampanou, D. Gentien, S. Saada, F. Assayag, A. Thuleau, F. Némati
Study supervision: O. Lantz, M.-H. Stern

References

1. Shields CL, Shields JA. Ocular melanoma: relatively rare but requiring respect. Clin Dermatol 2009;27:122–33.
2. Augsburger JJ, Correa ZM, Shaikh AH. Effectiveness of treatments for metastatic uveal melanoma. Am J Ophthalmol 2009;148: 119–27.
3. Sisley K, Rennie IG, Parsons MA, Jacques R, Hammond DW, Bell SM, et al. Abnormalities of chromosomes 3 and 8 in posterior uveal

melanoma correlate with prognosis. Genes Chromosomes Cancer 1997;19:22–8.
4. Onken MD, Worley LA, Ehlers JP, Harbour JW. Gene expression profiling in uveal melanoma reveals two molecular classes and predicts metastatic death. Cancer Res 2004;64:7205–9.
5. Augsburger JJ, Gamel JW. Clinical prognostic factors in patients with posterior uveal malignant melanoma. Cancer 1990;66:1596–600.

6. Couturier J, Saule S. Genetic determinants of uveal melanoma. Dev Ophthalmol 2011;49:150–65.

7. Kaiserman I, Amer R, Pe'er J. Liver function tests in metastatic uveal melanoma. Am J Ophthalmol 2004;137:236–43.

8. Servois V, Mariani P, Malhaire C, Petras S, Piperno-Neumann S, Plancher C, et al. Preoperative staging of liver metastases from uveal melanoma by magnetic resonance imaging (MRI) and fluorodeoxyglucose-positron emission tomography (FDG-PET). Eur J Surg Oncol 2010;36:189–94.

9. Mariani P, Piperno-Neumann S, Servois V, Berry MG, Dorval T, Plancher C, et al. Surgical management of liver metastases from uveal melanoma: 16 years' experience at the Institut Curie. Eur J Surg Oncol 2009;35:1192–7.

10. Schwarzenbach H, Hoon DS, Pantel K. Cell-free nucleic acids as biomarkers in cancer patients. Nat Rev Cancer 2011;11:426–37.

11. Diehl F, Li M, Dressman D, He Y, Shen D, Szabo S, et al. Detection and quantification of mutations in the plasma of patients with colorectal tumors. Proc Natl Acad Sci U S A 2005;102:16368–73.

12. Diehl F, Schmidt K, Choti MA, Romans K, Goodman S, Li M, et al. Circulating mutant DNA to assess tumor dynamics. Nat Med 2008;14:985–90.

13. Milbury CA, Li J, Makrigiorgos GM. PCR-based methods for the enrichment of minority alleles and mutations. Clin Chem 2009;55: 632–40.

14. Pekin D, Skhiri Y, Baret JC, Le Corre D, Mazutis L, Salem CB, et al. Quantitative and sensitive detection of rare mutations using droplet-based microfluidics. Lab Chip 2011;11:2156–66.

15. Hindson BJ, Ness KD, Masquelier DA, Belgrader P, Heredia NJ, Makarewicz AJ, et al. High-throughput droplet digital PCR system for absolute quantitation of DNA copy number. Anal Chem 2011;83: 8604–10.

16. Liu Q, Sommer SS. Pyrophosphorolysis-activated polymerization (PAP): application to allele-specific amplification. Biotechniques 2000;29:1072–6, 8, 80 passim.

17. Liu Q, Sommer SS. Detection of extremely rare alleles by bidirectional pyrophosphorolysis-activated polymerization allele-specific amplification (Bi-PAP-A): measurement of mutation load in mammalian tissues. Biotechniques 2004;36:156–66.

18. Liu Q, Sommer SS. PAP: detection of ultra rare mutations depends on P* oligonucleotides: "sleeping beauties" awakened by the kiss of pyrophosphorolysis. Hum Mutat 2004;23:426–36.

19. Van Raamsdonk CD, Bezrookove V, Green G, Bauer J, Gaugler L, O'Brien JM, et al. Frequent somatic mutations of GNAQ in uveal melanoma and blue naevi. Nature 2009;457:599–602.

20. Van Raamsdonk CD, Griewank KG, Crosby MB, Garrido MC, Vemula S, Wiesner T, et al. Mutations in GNA11 in uveal melanoma. N Engl J Med 2010;363:2191–9.

21. Bauer J, Kilic E, Vaarwater J, Bastian BC, Garbe C, de Klein A. Oncogenic GNAQ mutations are not correlated with disease-free survival in uveal melanoma. Br J Cancer 2009;101:813–5.

22. Nemati F, Sastre-Garau X, Laurent C, Couturier J, Mariani P, Desjardins L, et al. Establishment and characterization of a panel of human uveal melanoma xenografts derived from primary and/or metastatic tumors. Clin Cancer Res 2010;16:2352–62.

23. Rago C, Huso DL, Diehl F, Karim B, Liu G, Papadopoulos N, et al. Serial assessment of human tumor burdens in mice by the analysis of circulating DNA. Cancer Res 2007;67:9364–70.

24. Mouliere F, Robert B, Arnau Peyrotte E, Del Rio M, Ychou M, Molina F, et al. High fragmentation characterizes tumour-derived circulating DNA. PLoS One 2011;6:e23418.

25. Keilholz U, Goldin-Lang P, Bechrakis NE, Max N, Letsch A, Schmittel A, et al. Quantitative detection of circulating tumor cells in cutaneous and ocular melanoma and quality assessment by real-time reverse transcriptase-polymerase chain reaction. Clin Cancer Res 2004;10: 1605–12.

26. Schuster R, Bechrakis NE, Stroux A, Busse A, Schmittel A, Thiel E, et al. Prognostic relevance of circulating tumor cells in metastatic uveal melanoma. Oncology 2011;80:57–62.

27. Ulmer A, Beutel J, Susskind D, Hilgers RD, Ziemssen F, Luke M, et al. Visualization of circulating melanoma cells in peripheral blood of patients with primary uveal melanoma. Clin Cancer Res 2008;14: 4469–74.

28. Mariani P, Dorval T, Neel N, Kavian N, Piperno-Neuman S, Asselain B, et al. Absence of detectable tumoral cells in the blood or bone marrow of ocular melanoma patients operated for liver metastasis. EJC Supplements 2009;7:587–8.

Clinical Cancer Research

Pyrophosphorolysis-Activated Polymerization Detects Circulating Tumor DNA in Metastatic Uveal Melanoma

Jordan Madic, Sophie Piperno-Neumann, Vincent Servois, et al.

Updated version	Access the most recent version of this article at: doi:10.1158/1078-0432.CCR-12-0309
Supplementary Material	Access the most recent supplemental material at: http://clincancerres.aacrjournals.org/content/suppl/2012/05/29/1078-0432.CCR-12-0309.DC1

Cited articles	This article cites 28 articles, 7 of which you can access for free at: http://clincancerres.aacrjournals.org/content/18/14/3934.full#ref-list-1
Citing articles	This article has been cited by 5 HighWire-hosted articles. Access the articles at: http://clincancerres.aacrjournals.org/content/18/14/3934.full#related-urls

E-mail alerts	Sign up to receive free email-alerts related to this article or journal.
Reprints and Subscriptions	To order reprints of this article or to subscribe to the journal, contact the AACR Publications Department at pubs@aacr.org.
Permissions	To request permission to re-use all or part of this article, use this link http://clincancerres.aacrjournals.org/content/18/14/3934. Click on "Request Permissions" which will take you to the Copyright Clearance Center's (CCC) Rightslink site.